

Chaotic Colpitts Oscillator

F. R. Tahir,

*Department of Electrical Engineering, College of Engineering,
University of Basrah,
Basrah – Iraq*

ISSN -1817 -2695

Received 18/8/2006, Accepted 1/11/2006

Abstract:

Studies of chaos in electronic circuits and systems have shown that chaotic signals generated in these systems can potentially be used as carriers for information transmission in the communications systems. This paper demonstrates the generation of chaos in the Colpitts oscillator by using numerical simulation. The dynamics of the different voltages and the current through the inductor are calculated when the series resistance with inductor taken as a bifurcation element. The values of the emitter resistance that generate the chaotic behavior is investigated. The generation of chaos is confirmed by calculating the bifurcation diagram, phase portrait attractors, and three dimensional- attractors. The bifurcation diagram allows the classification of the regions of the different behaviors of oscillator (quasi-periodic oscillations and chaotic oscillations).

Key words:- Colpitts Oscillator, Chaos, Bifurcation.

I-Introduction:

Recently, an increase interest in studying the behavior of nonlinear dynamics of electronic circuits. Many electronic circuits are capable of generating chaos. The chaotic signal can be useful in applications such as transmitting information, signal encryption, and secure communications systems [1-4]. Chaotic electronic oscillators used for communications require specific characteristics such as a broadband, security, and low interference code generation. One of the good candidates of chaotic electronic circuits for communications is the Colpitts oscillator. Nonlinear dynamics in Colpitts oscillator has been intensively investigated for several years [5-7].

In this paper, the chaotic oscillations in Colpitts oscillator are numerically investigated. The paper's structure is as follows. In section II some background information about the Colpitts oscillator is given and the circuit model is introduced. The simulation results are presented in section III. Section IV provides a short summary and conclusions.

II- Colpitts oscillator: Circuit modeling

The Schematic diagram of the Colpitts oscillator is shown in Fig.(1). The circuit comprises a single bipolar junction transistor (BJT), acting as the gain element, and a resonant network consisting of an inductor (L) and a pair of capacitors (C1 and C2). Supply voltages Vcc and Vee provide the circuit bias [8].

The circuit can be described by the following three state equations:

$$C1 \frac{dV_{ce}}{dt} = I_L - \beta_f F(V_{be}) \quad \dots(1)$$

$$C2 \frac{dV_{be}}{dt} = -I_L - F(V_{be}) - \frac{1}{R_e} V_{be} + \frac{V_{ee}}{R_e} \quad \dots(2)$$

$$L \frac{dI_L}{dt} = -R_L I_L - V_{ce} + V_{be} + V_{cc} \quad \dots(3)$$

where the state variables are $V_{ce}(= V_{c1})$ is the voltage difference between collector and emitter of the transistor, $V_{be}(= -V_{c2})$ is the voltage difference between base and emitter of the transistor, and I_L is the current through the inductor L . $F(.)$ is the characteristic of the transistor and can be modeled as follows [9]:

$$F(V_{be}) = \begin{cases} 0, & V_{be} \leq V_{th} \\ \frac{V_{be} - V_{th}}{R_{on}}, & V_{be} > V_{th} \end{cases} \quad \dots(4)$$

where, V_{th} is the threshold voltage of base – emitter junction, R_{on} is the small signal on – resistance of the base-emitter junction, and $\beta_f(= h_{fe})$ is the forward current gain of the transistor.

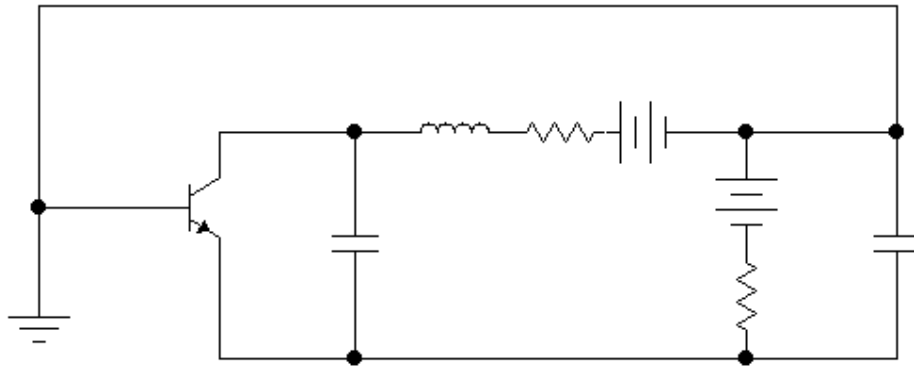


Fig. (1): Schematic diagram of Colpitts oscillator.

III-Simulation results:

The calculations of the dynamics of the chaotic oscillations achieved with parameters values are listed in table I.

The bifurcation diagram of the temporal waveforms of collector voltage $V_c(= V_{ce} - V_{be})$ when the inductor series resistance R_L is decreased from 46 to 3.0 Ω is shown in Fig.(2). The peak values of the temporal waveform are sampled and plotted as a function of R_L . As R_L is decreased, quasi-periodic oscillations are observed from $R_L=46$ to 39 Ω . When R_L is decreased below 39 Ω the peak values distributing region is increased and the chaotic oscillations are observed. From $R_L=13$ to 3.0 Ω the peak values distributed in broad region and quasi-periodic oscillations are observed again.

Fig.(3) depicts the temporal waveforms of the collector voltage V_c , emitter voltage $V_e (= -V_{be})$, and the inductor current I_L when R_L is varied. At $R_L = 15 \Omega$, quasi-periodic oscillations are observed for voltages and current as shown in Fig.(3a). The temporal waveforms oscillations become more chaotic as R_L is increased. They fluctuate chaotically at $R_L = 26 \Omega$ as shown in Fig.(3b). The waveforms become quasi-periodic oscillations again as shown in Fig.(3c) ($R_L = 40 \Omega$). Fig.(4) demonstrates the observed V_c - V_e phase portrait scroll attractors at the values of R_L (15Ω , 26Ω , and 40Ω , respectively).

Also, the three dimensional (3D) - attractors in phase space of the voltages, V_c and V_e , and the current I_L are obtained. Fig.(5) shows the 3D – attractors at different values of R_L . For $R_L = 15 \Omega$, quasi-periodic oscillations are observed as shown in Fig.(5a). A chaotic attractor is observed at $R_L = 26 \Omega$ as shown in Fig.(5b). Another, quasi-periodic attractor is reproduced as shown in Fig.(5c) ($R_L = 40 \Omega$).

Fig.(6)(A, B, and C) display, respectively, the dependence of the phase portrait scroll attractors state on the values of the emitter resistance R_e , while the resistance R_L is fixed at the selected value. The results reveal that the following remarks:

- By increasing the resistance R_e , the attractor leaves the quasi-periodic state regime and becomes chaotic state.
- A rich chaotic state can be obtained by assign specific values to resistance R_L and increasing the emitter resistance R_e as shown in Fig.(6)B.
- It is worth emphasis that the values of the emitter resistance R_e also affect the attractor state and therefore, can be used as a bifurcation element.

Table I: Parameters values used in simulations

| Parameter | Value |
|----------------------|------------------|
| C1 | 57 [nF] |
| C2 | 58 [nF] |
| L | 100 [μ H] |
| R_e | 385 [Ω] |
| R_L | variable |
| R_{on} | 375 [Ω] |
| V_{cc} | + 5 [v] |
| V_{ee} | + 5 [v] |
| $\beta_f (= h_{fe})$ | 140 |
| V_{th} | 0.75 [v] |
| Q | 2SC1740 |

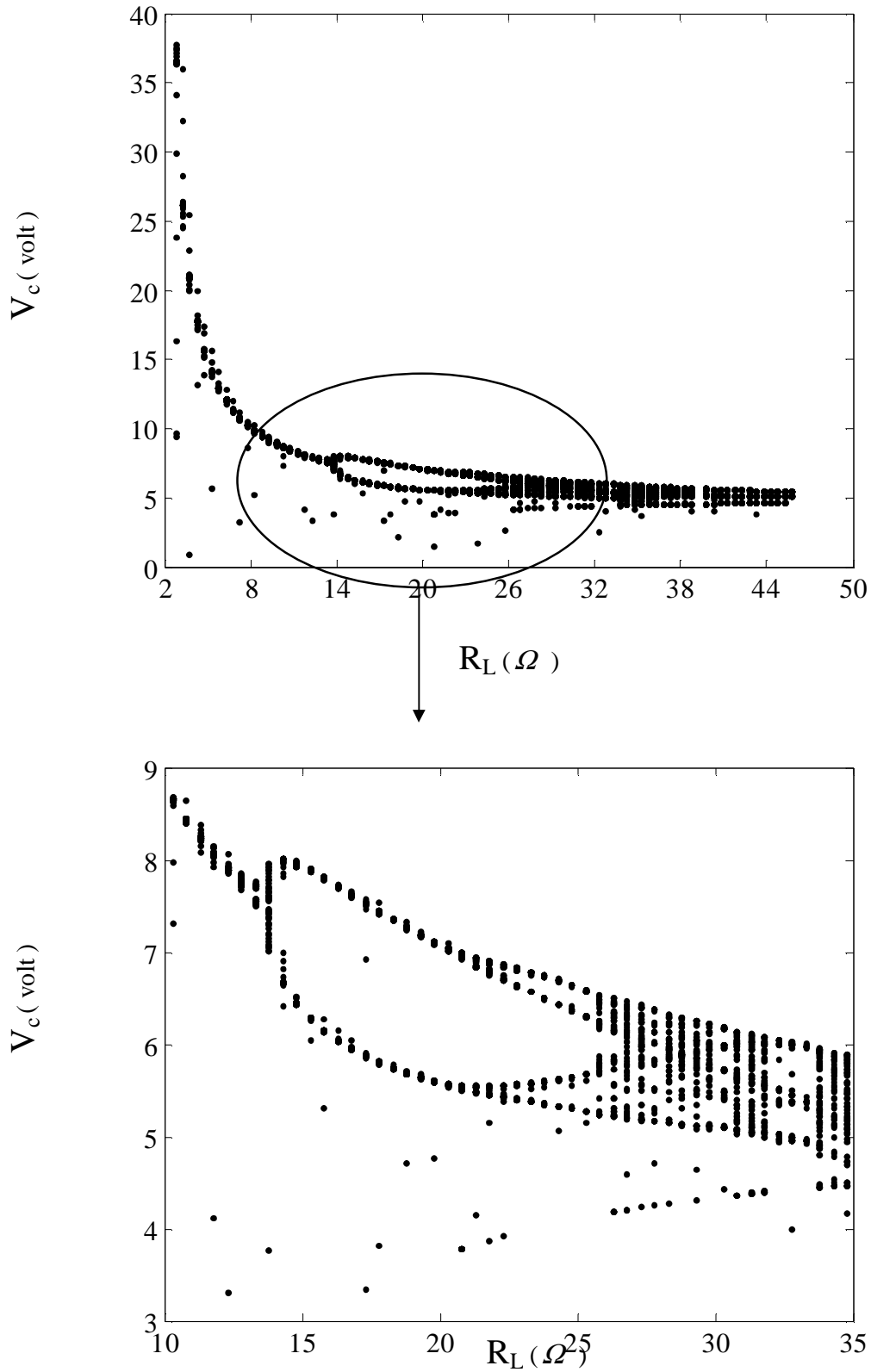


Figure (2): Bifurcation diagram of temporal waveform of collector voltage V_c when R_L decrease from 46 to 3 Ω

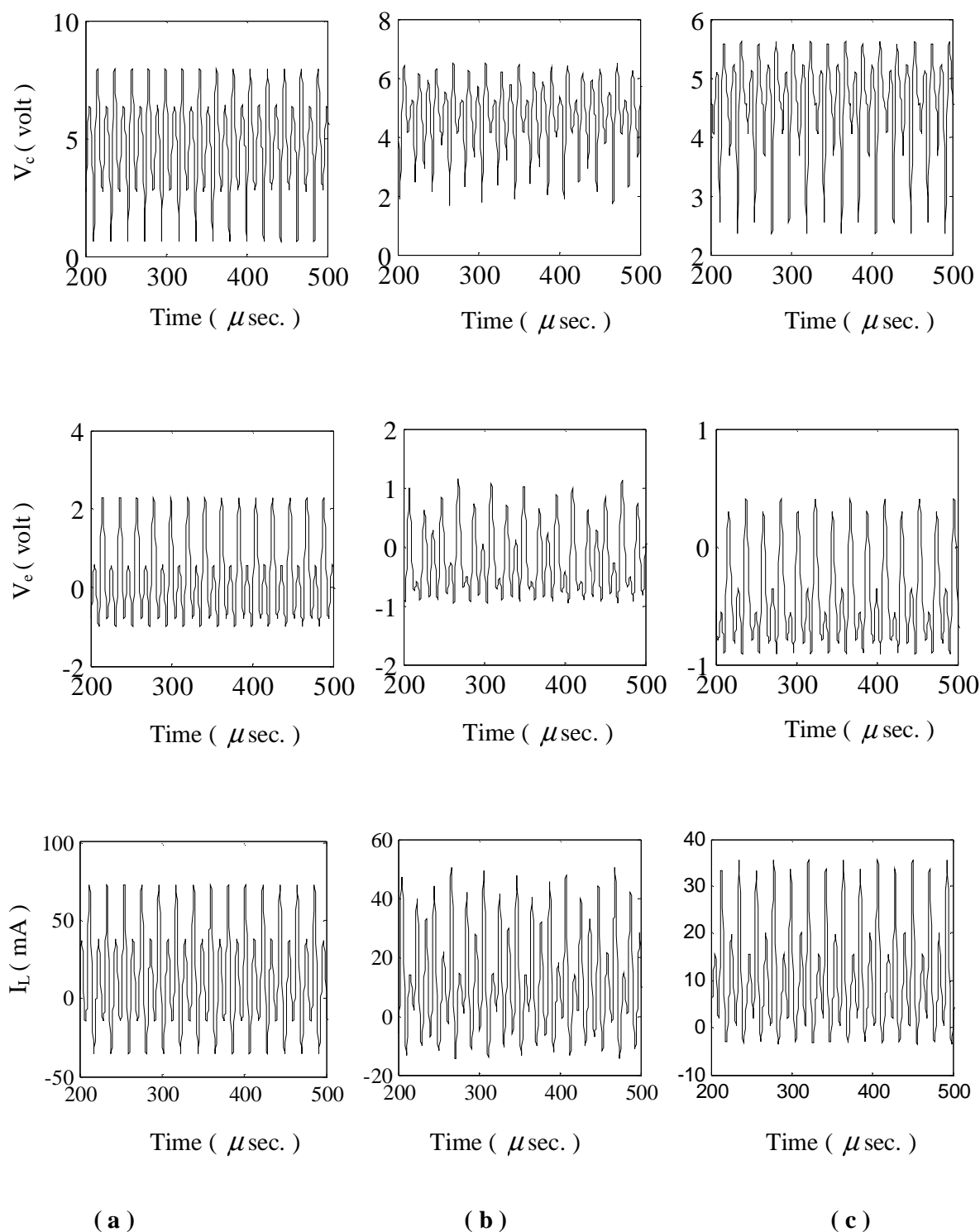


Figure (3): Top to bottom: temporal waveforms of collector voltage, emitter voltage, and inductor current at different values of R_L : (a) $R_L = 15 \Omega$, (b) $R_L = 26 \Omega$, and (c) $R_L = 40 \Omega$

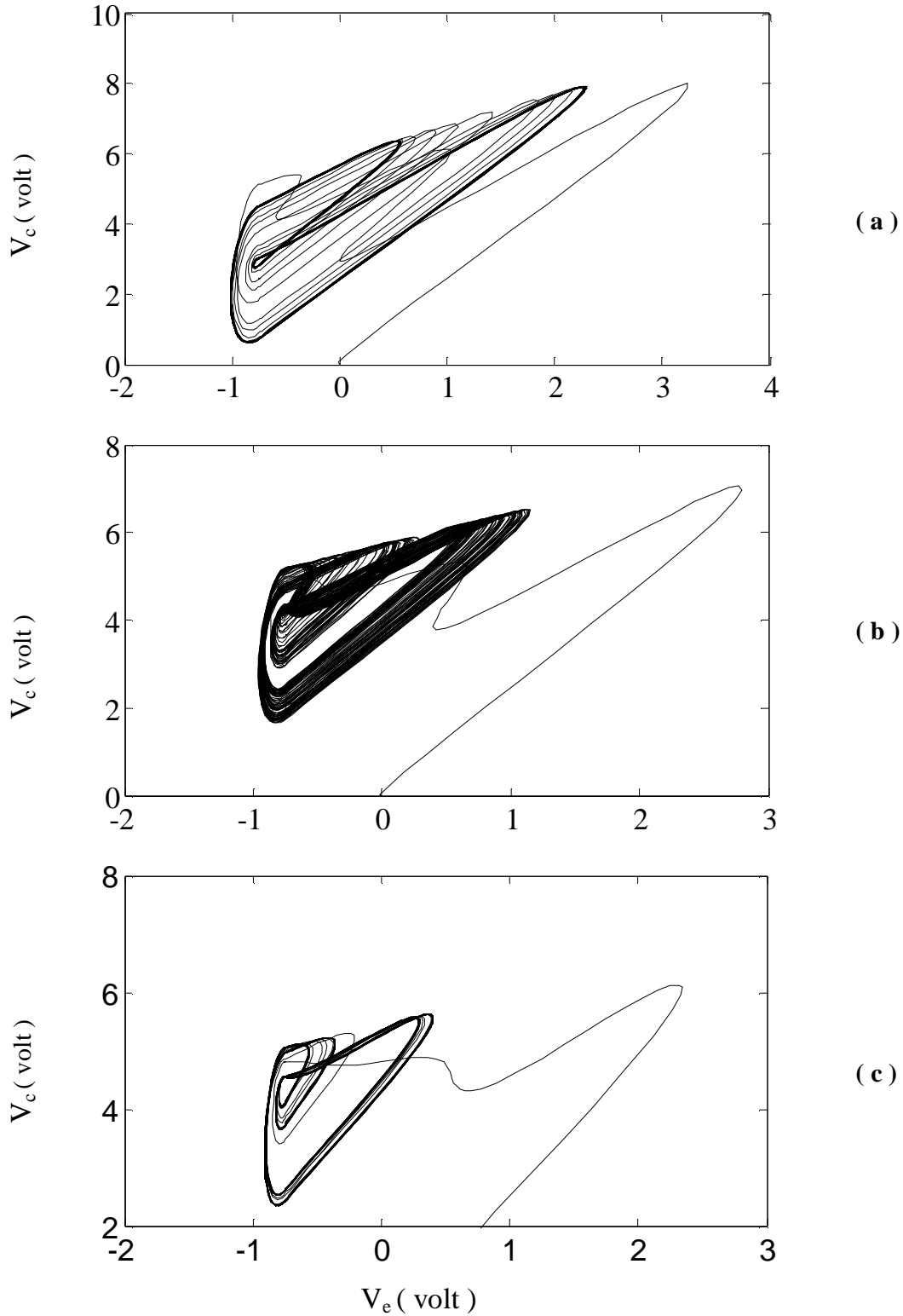


Figure (4): Phase portrait scroll attractors of collector voltage vs. emitter voltage at different values of R_L : (a) $R_L = 15 \, \Omega$, (b) $R_L = 26 \, \Omega$, and (c) $R_L = 40 \, \Omega$

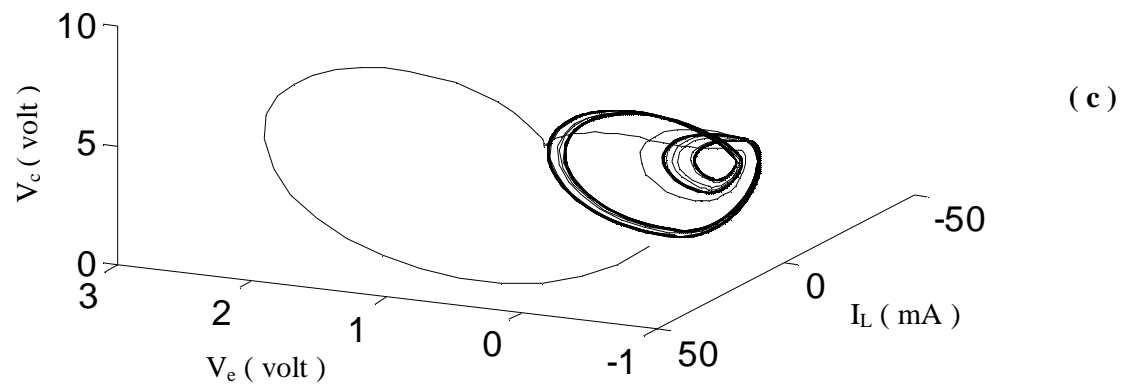
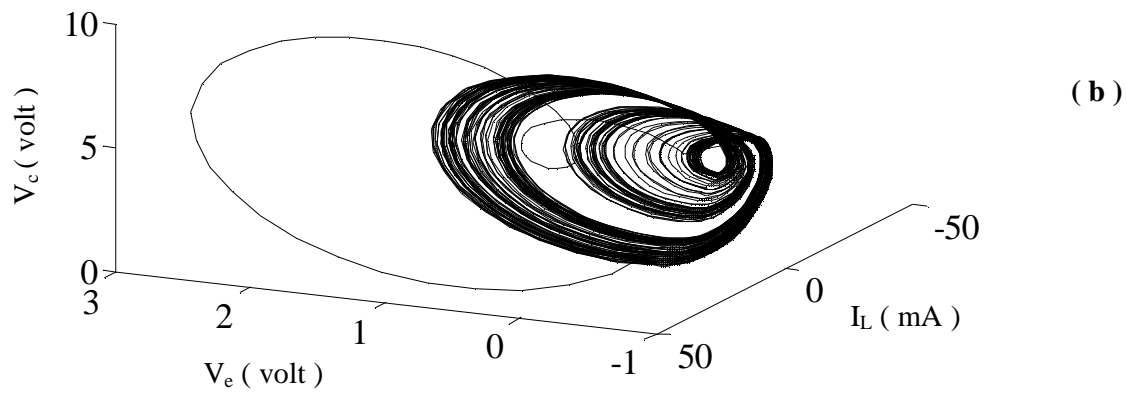
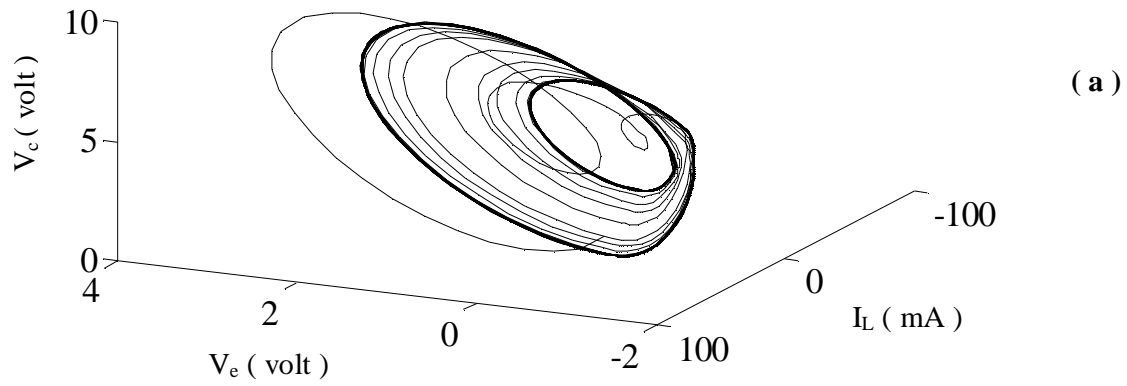


Figure (5): 3D - attractors at different values of R_L : (a) $R_L = 15 \, \Omega$, (b) $R_L = 26 \, \Omega$, and (c) $R_L = 40 \, \Omega$

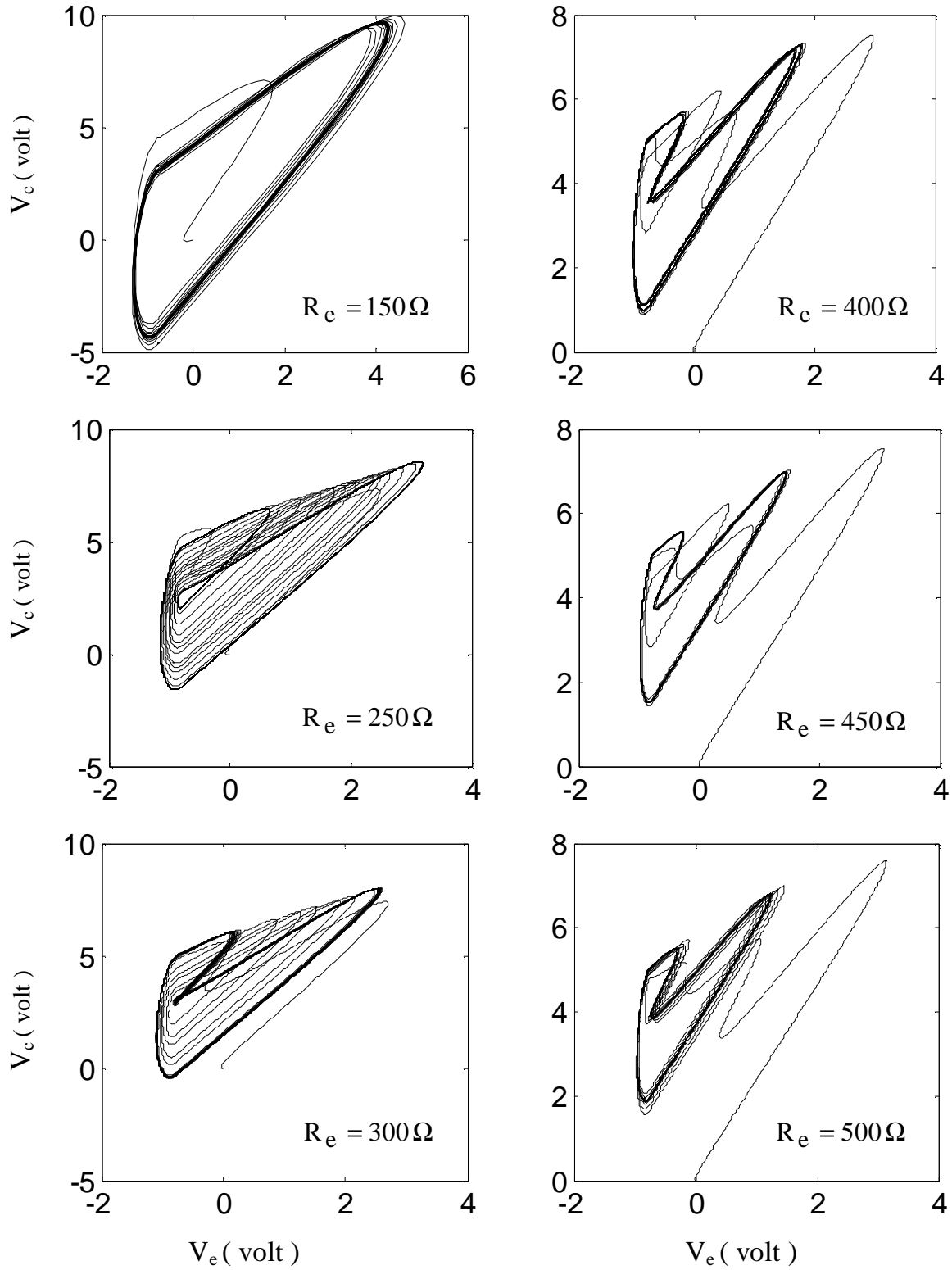


Figure (6): A- Phase portrait scroll attractors of collector voltage vs. emitter voltage. The resistance R_L is fixed at 20Ω , while R_e is increased

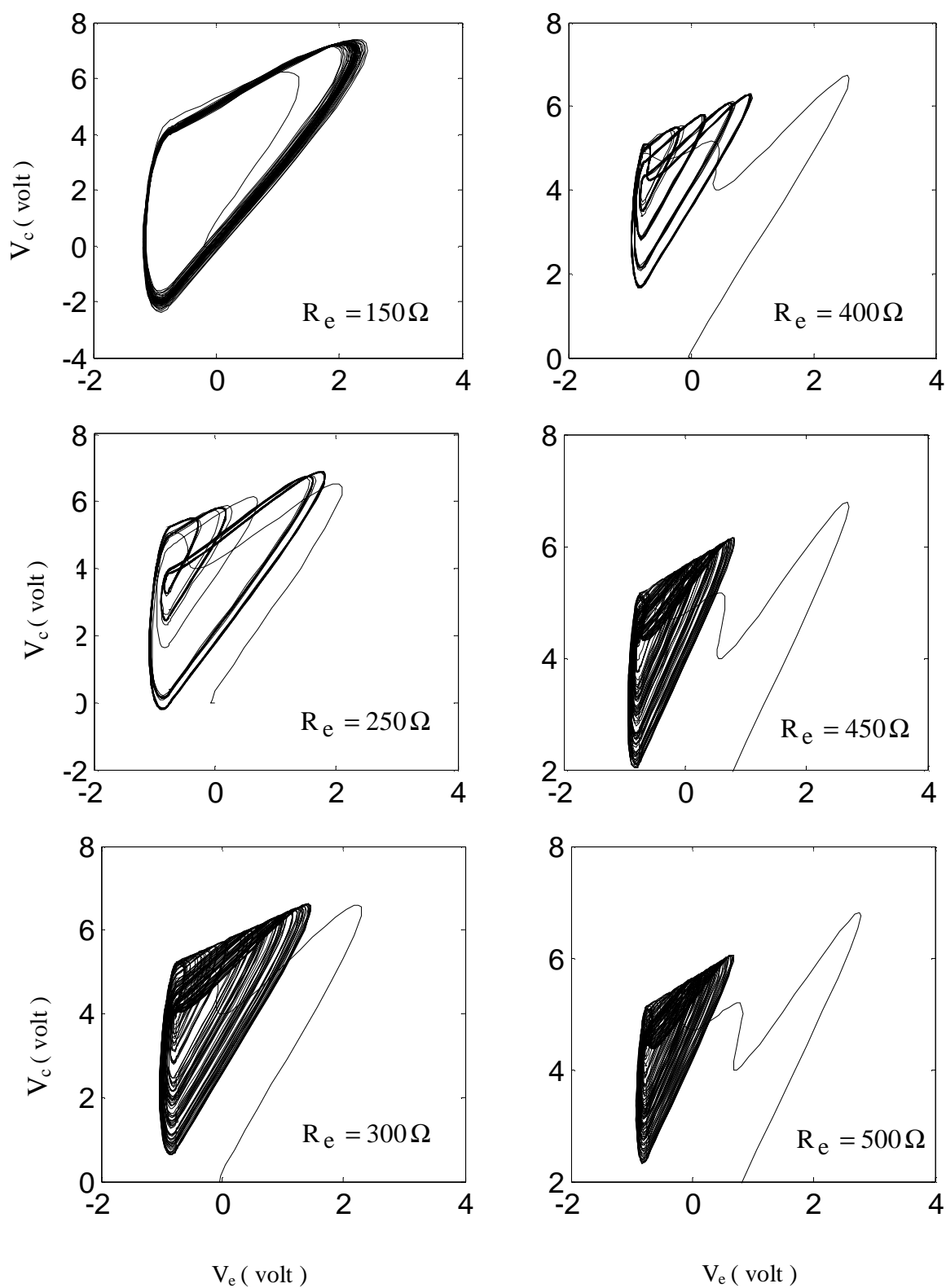


Figure (6): (Continued) B- The resistance R_L is fixed at 30Ω

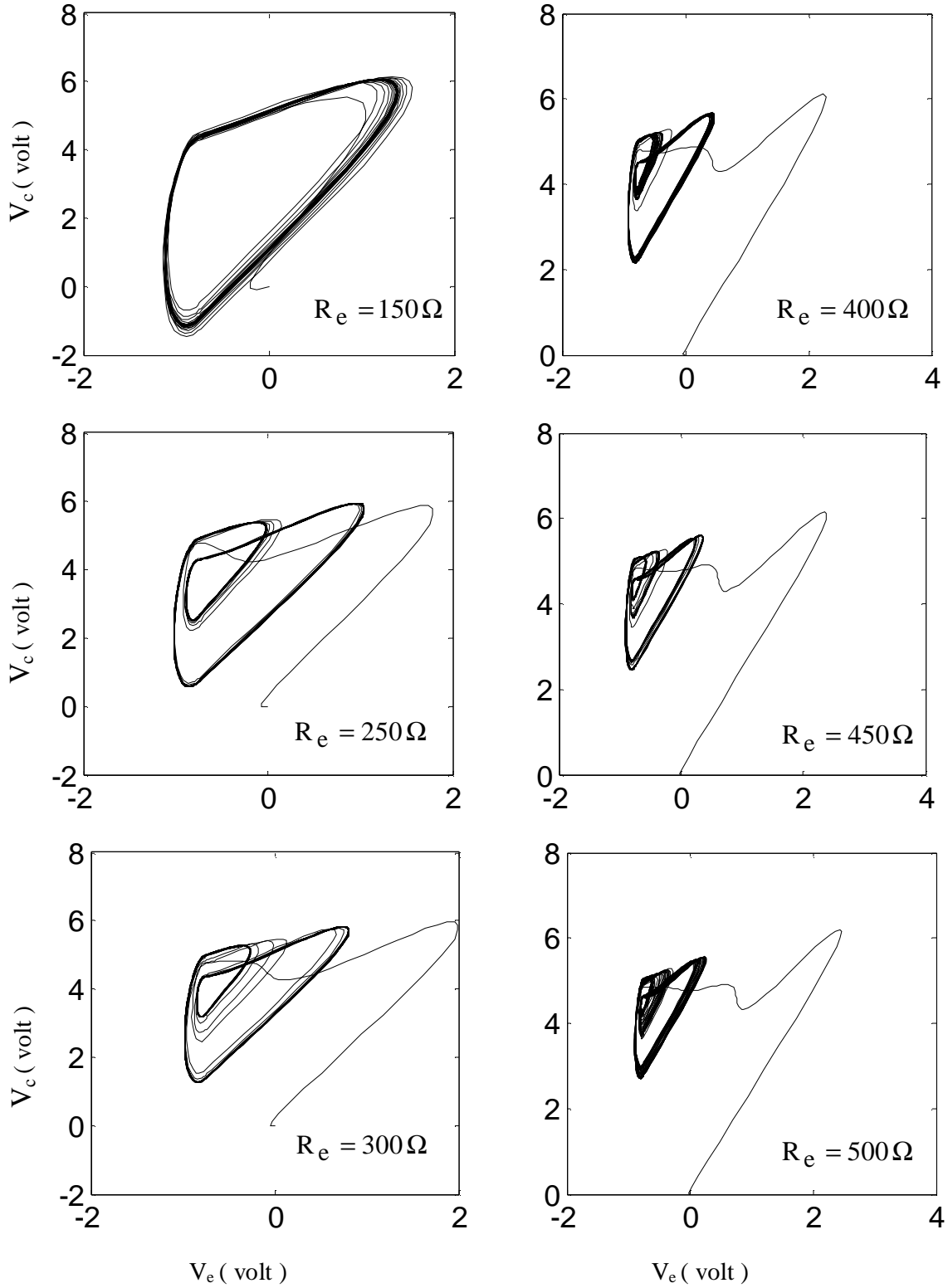


Figure (6): (Continued) C- The resistance R_L is fixed at 40Ω

IV – Conclusions:

The dynamics of an autonomous electronic circuit, namely Colpitts oscillator, is calculated. As the inductor series resistance decreases, a quasi-periodic attractor breaks down and a chaotic attractor appears. This bifurcation diagram can be interpreted as the quasi-periodicity-breakdown to chaos. The bifurcation diagram, phase portrait scroll attractors, and 3D - attractors confirm the generation of chaos behavior.

References:

- [1] S.A. Mahmoud, A. S. Elwakil, and A. M. Soliman, INT. j. electronics, 12 , 1441, (1999).
- [2] Y. V. Andreyev, A. S. Dmitriev, E. V. Efremova, A. D. Khilinsky, and L. V. Kuzmin, International journal of bifurcation and chaos, 11, 3639, (2005).
- [3] E. Freire, L. G. Franquelo, and J. Aracil, IEEE transactions on circuits and systems, 3,. 237, (1984).
- [4] T. Endo, and L. O. Chua, IEEE transactions on circuits and systems, 8, 987,(1988).
- [5] A. Uchida, M. Kawano, and S. Yoshimori, Physical review E 68, 056207, (2003).
- [6] A. Uchida, K. Takahashi, M. Kawano, and S. Yoshimori, IEICE trans. fundamentals, 9, 2072, (2002).
- [7] G. M. Maggio, O. D. Feo, and M. P. Kennedy, IEEE transactions on circuits and systems – I: fundamental theory and applications, 9, 1118, (1999).
- [8] O. D. Feo, G. M. Maggio, and M. P. Kennedy, International journal of bifurcation and chaos, 5, 935, (2000).
- [9] N. F. Rulkov, and A. R. Volkovskii, IEEE transactions on circuits and systems – I: fundamental theory and applications, 6, 673, (2001).

مذبذب كولبيتس التخبطي

فاضل رحمة طاهر

قسم الهندسة الكهربائية, كلية الهندسة, جامعة البصرة

البصرة – العراق

الخلاصة:

دراسة التخبط في الدوائر الالكترونية والأنظمة تُظهر إمكانية استخدام الإشارات التخبطية المتولدة من تلك الأنظمة كحاملات (carriers) لنقل المعلومات في أنظمة الاتصالات. هذا البحث يُبرهن توليد السلوك التخبطي في مذبذب كولبيتس (Colpitts oscillator) باستخدام المحاكاة العددية (numerical simulation). ديناميكية الفولتيات المختلفة في المذبذب والتيار المار بالمحاث حُسِبَت بأخذ المقاومة المتوالية مع المحاث كعنصر مُشعَب (bifurcation element). تم التحقق من قيم مقاومة الباعث للترانزستور (emitter resistance) التي تقود إلى السلوك التخبطي. توليد التخبط تأكد بحساب: الرسم التخبطي للتشعَب (bifurcation diagram), مسقط للجاذبات (attractors), و رسم ثلاثي الأبعاد للجاذبات. الرسم التخبطي للتشعَب يسمح بتصنيف المناطق المختلفة لتصرف المذبذب, مثل التذبذب الدوري إلى درجة ما (oscillations) و التذبذب التخبطي (chaotic oscillation)

